ELSEVIER

Thermochimica Acta 384 (2002) 101–111

thermochimica acta

www.elsevier.com/locate/tca

Thermal decomposition of 2,2-bis(difluoroamino) propane studied by FTIR spectrometry and quantum chemical calculations: the primary dissociation kinetics and the mechanism for decomposition of the $(CH_3)_2CNF_2$ radical

J. Park[a], D. Chakraborty[a], S. Jamindar[a], W.S. Xia[a], M.C. Lin[a,*], C. Bedford[b]

[a]*Department of Chemistry, Emory University, Atlanta, GA 30322, USA*
[b]*Weapons Division, Naval Air Warfare Center, China Lake, CA, USA*

Abstract

The kinetics of the thermal decomposition of 2,2-bis(difluoroamino) propane (BDFP) has been studied by pyrolysis/FTIR spectrometry at temperatures between 528 and 553 K using toluene as radical scavenger. The disappearance of BDFP was found to follow the first-order kinetics with the rate constant, $k_1 = 10^{16.0\pm0.7} \exp[-(24200 \pm 840)/T]\ s^{-1}$, which agrees closely with the expression obtained by Fokin et al. [Dokl. Akad. Nauk. 332 (1993) 735], $k_1 = 10^{15.60} \exp(-23600/T)\ s^{-1}$. The measured large A-factor supports the earlier conclusion that the primary fragmentation process corresponds to the breaking of one of the two NF_2 groups. The measured activation energy is also consistent with the predicted first C–N bond dissociation energy, 44–48 kcal/mol, by the hybrid density-functional theory and that evaluated by variational RRKM calculations fitting the observed rate constant, 47.9 kcal/mol. The 2-difluoroamino propyl radical, $(CH_3)_2CNF_2$, was predicted to be thermally unstable, producing readily F atoms and HF molecules via the $(CH_3)_2CFNF$ intermediate. The quantum-chemically predicted mechanisms for the fragmentation of $(CH_3)_2C(NF_2)_2$ and $(CH_3)_2CNF_2$ agree with the product distribution reported by Ross and coworkers [J. Am. Chem. Soc. 94 (1972) 8776].

Keywords: Thermal decomposition; 2,2-Bis(difluoroamino) propane; Propellants

1. Introduction

The oxidizing nitro group increases the density of propellants and explosives and promotes the formation of very stable gaseous decomposition products (N_2, CO, CO_2 and H_2O) through fast, exothermic redox reactions, resulting in a large energy release and pressure buildup per unit volume of material. Replacing some $–NO_2$ groups by $–NF_2$, the difluoroamino group, it is possible to improve both the amount and the rate of energy release in energetic material systems such as propellants.

Recently Lane and Politzer [1] discussed the replacement of some $–NO_2$ groups by $–NF_2$. They concluded that the compound's density and the number of moles of gaseous combustion products formed per gram of material can be increased, thereby enhancing propellant performance. Thus, in designing energetic molecules (i.e. explosives and propellants), it can be advantageous to include some difluoroamine groups along with the usual nitro group.

* Corresponding author. Tel.: +1-404-727-2825; fax: +404-727-6586.
E-mail address: chemmcl@emory.edu (M.C. Lin).

0040-6031/02/$ – see front matter
PII: S0040-6031(01)00781-X

In order to understand the complex mechanism for the thermal decomposition of a potential energetic compound, 4,4-bis(difluoroamino)-1-nitropiperidine, [2] we consider the thermal decomposition of a model compound of 2,2-bis(difluoroamino) propane (BDFP) in the present study. Earlier theoretical studies based on some mono-difluoroamines [3] showed that HF elimination through a four-centered transition state is energetically more favorable than the initial rupture of an N–F bond. Also, when all α-hydrogens are replaced by methyl groups, N–F dissociation energy increases slightly but undesirable destabilization due to HF elimination can be avoided. On the other hand, C–N bond dissociation energies in some related systems (containing α-hydrogen) were observed to be ∼65 kcal/mol [1,4]. Thus, in the present model compound, BDFP, HF elimination might not be favorable due to the absence of α-hydrogens; instead, C–N or N–F bond cleavage might be the rate-controlling process.

Two earlier experimental studies [5,6] on the decomposition of BDFP indeed indicated that the initial products of the reaction measured at 723 and 1023 K under low-pressure conditions derived primarily from the first C–NF_2 bond scission with 45 kcal/mol activation energy, [5] which is in close agreement with the value, 47 kcal/mol, reported by Fokin et al. [6] based on the BDFP decay rate determination at lower temperatures. These results will be referred to later in the discussion on the kinetics and mechanism of the BDFP decomposition reaction.

Our present objective is to examine the mechanism for the initial decomposition of the bis-difluoroamino compound and to evaluate the rate constant for the unimolecular decomposition process, aided by quantum and statistical-theory calculations, in order to shed some light on the mechanism for the thermal decomposition of larger bis-difluoroaminonitramine propellants.

2. Experimental details

2.1. Preparation of BDFP

BDFP was prepared at NAWL, China Lake, CA, using the procedure similar to that of Baum [7] for the difluoroamination of acetone. Acetone (4.5 g, 0.078 mol) was added drop-wise with stirring to a cold suspension of 17.6 g of difluoroamine in 30% oleum. After 2 h, the reaction mixture was treated with toluene and the organic layer was separated. The organic extract was distilled at atmospheric pressure, yielding approximately a 1:1 mixture of BDFP: toluene, bp 80–85 °C. The proton and fluorine NMR spectra were consistent with previously reported values [7].

For general information, an excellent description of the experimental procedure and the reaction set-up of difluoroamination by Chapman et al. [8] is available. Difluoroamine was generated by acidic hydrolysis of *N*,*N*-difluorourea, prepared by direct fluorination of aqueous urea. [9,10] Since difluoroamine under certain conditions can be an extremely sensitive and detonable material, [11–13] adequate shielding should be used to contain a possible detonation.

2.2. Kinetic measurements

The thermal decomposition of BDFP in toluene was carried out in a 270 ml quartz reactor placed in a well-insulated double-walled cylindrical furnace. The reaction temperature was measured using a thermocouple placed at the center of the reactor and connected to a temperature controller, which maintained the temperature within 1 K during the experiment. The thermocouple had been calibrated at the freezing point and boiling point of water before use. The reactor was directly connected to a gas-handling system and to a FTIR sample tube. Four different mixtures with varying amounts of BDFP, toluene and H_2O diluted with argon were used in the present studies. The reactions were carried out at nine different temperatures in the range of 528–553 K at a constant total pressure of 760 Torr, in order to minimize surface effects. Both unpyrolyzed and pyrolyzed mixtures were analyzed by FTIR spectrometry (Mattson Instruments Polaris Spectrometer), using 7 in. long and 1 in. o.d. sample cell sealed with KCl windows. The analysis cell is directly attached to the reaction system through 3/4 in. o.d. Teflon tubing. After expansion from the reactor at 760 Torr initial pressure, the sample pressure was typically ∼300 Torr. Accordingly, all calibrations were performed with ∼300 Torr standard mixtures containing various amounts of BDFP. Since original samples came with toluene, calibration of toluene was also performed in order to obtain the exact concentrations of BDFP in the reaction mixtures. The strong infrared

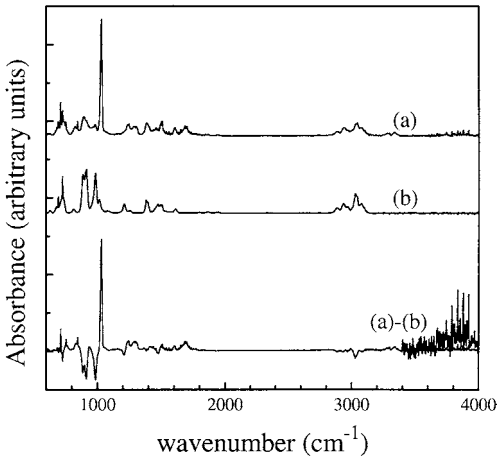

Fig. 1. Typical FTIR spectra of pyrolyzed (a) and unpyrolyzed (b) BDFP in mixture I. HF spectra above 3800 cm^{-1} were expanded for better visibility.

Table 1
The experimental conditions and measured first-order rate constants for the unimolecular decomposition of BDFP at various temperatures

T (K)	Mixture[a]	k_1 (s^{-1})
528	II	1.1×10^{-4}
533	I	1.8×10^{-4}
536	III	2.1×10^{-4}
538	II	2.3×10^{-4}
541	III	3.4×10^{-4}
543	I	4.3×10^{-4}
543	IV	4.1×10^{-4}
548	II	5.5×10^{-4}
550	III	7.1×10^{-4}
553	I	8.6×10^{-4}

[a] Mixture: (I), 0.1306% of BDFP and 0.1489% of toluene in argon; (II), 0.0544% of BDFP and 2.442% of toluene in argon; (III), 0.0464% of BDFP and 2.081% of toluene in argon; (IV), 0.0458% of BDFP, 2.054% of toluene and 1.315% H_2O in argon.

bands at 985 and 729 cm^{-1} were used to calibrate the concentrations of the BDFP and toluene, respectively.

3. Results and discussion

3.1. Pyrolytic study

The thermal decomposition of BDFP has been studied with various mixtures at nine different temperatures in the range 528–553 K while maintaining a constant total pressure of 760 Torr. Fig. 1 presents a typical absorption spectral profile of pyrolyzed and unpyrolyzed samples and Table 1 summarizes our experimental conditions and results. Two strong peaks at 1030 and 713 cm^{-1} are found as products from the pyrolyzed spectra by FTIR analysis and identified as SiF_4 and HCN, respectively. Complex spectra in the region above 3800 cm^{-1} confirmed [14] the formation of HF in the present decomposition reaction. Formation of SiF_4 may be caused by the reaction of HF and SiO_2 (from reactor quartz wall). Since H_2O is formed by the reaction of HF and SiO_2, a mixture of 0.0458% BDFP in toluene with excess H_2O (1.3%) is also pyrolyzed to study the effect of H_2O on the initiation of the decomposition reaction. The addition of 1.3% H_2O eliminated SiF_4 through hydrolysis, but was found to have no effect on the reactant decay rate (see Table 1). Thus, HF and HCN are potentially the major products in this thermal decomposition reaction. Effort to identify other organic products is underway with the help of quantum chemical calculations.

Fig. 2 shows the decay of BDFP concentration and the rise of SiF_4 peak intensity. Under the experimental conditions, the BDFP decay data show that the rate of its decomposition follows the first-order rate law.

With the first-order kinetics for the decomposition in the gas phase,

$$A \xrightarrow{k_1} B + C$$

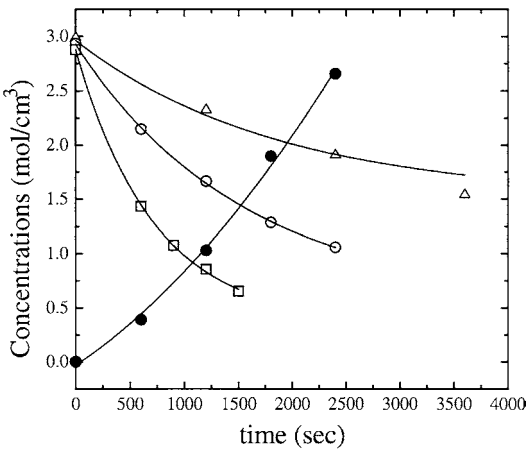

Fig. 2. Typical concentration profiles of BDFP at 533 K (△), 543 K (○), 553 K (□) and rise of peak intensity of SiF_4 (●) at 543 K using mixture I.

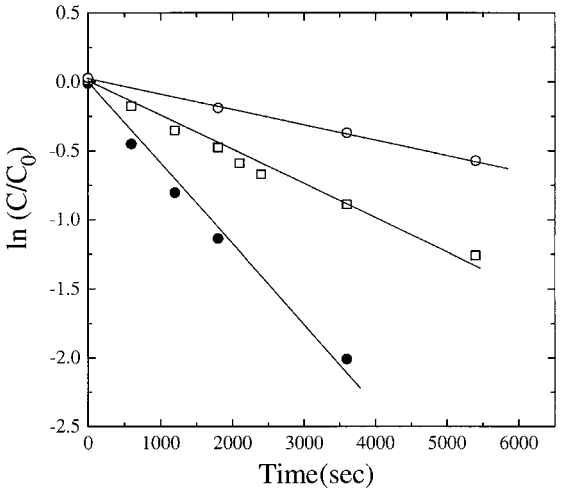

Fig. 3. First-order decay plots of BDFP at 528 K (○), 538 K (□) and 548 K (●) using mixture II.

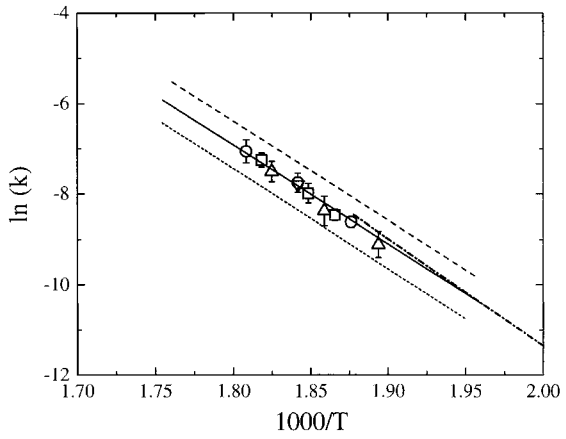

Fig. 4. Arrhenius plot for the rate constants obtained under various reaction conditions using (○) mixture I, (△) mixture II, (□) mixture III, and (▽) mixture IV. Solid line, predicted value from Variflex calculation with $E_0 = 47.9$ kcal/mol; dotted and dashed lines, predicted values from Variflex calculations with $E_0 = 47.9 \pm 0.1$ kcal/mol; dash-dotted line, Ref. [6].

$$\frac{\mathrm{d[A]}}{\mathrm{d}t} = -k_1[\mathrm{A}],$$

$$\ln[\mathrm{A}]_t = \ln[\mathrm{A}_0] - k_1 t,$$

k_1, the first-order rate constant, can be obtained from the slope of $\ln[\mathrm{A}]_t$ versus time plot.

Fig. 3 illustrates the first-order decay plots for the three different temperatures with mixture II. Table 1 summarizes the initial reaction conditions and the measured rate constants.

The rate constants are also graphically shown in Fig. 4 for the temperature range 528–553 K. A least-squares analysis of all the data based on the BDFP decay gave

$$k_1 = 10^{16.0\pm0.7} \exp\left[\frac{-(24200 \pm 840)}{T}\right] \mathrm{s}^{-1}$$

This result agrees closely with the expression reported by Fokin et al. [6] $k_1 = 10^{15.60} \exp(-23600/T)\ \mathrm{s}^{-1}$ obtained in the temperature range 493–533 K at BDFP pressures between 20 and 150 Torr in terms of both the A-factor and the activation energy. Their result is also included in Fig. 4 for comparison. Our activation energy, 48.1 ± 1.7 kcal/mol, also agrees reasonably with the value obtained at two temperatures (923 and 1023 K) under low-pressure conditions by Ross et al. [5] 45 kcal/mol. The high A-factor ($\sim 10^{16}\ \mathrm{s}^{-1}$) clearly supports the conclusion reached earlier [5,6] that the thermal decomposition is mainly controlled by the homolytic cleavage of one of the C–N bonds leading to the formation of $(CH_3)_2C(NF_2)$ and NF_2 radicals. Since there is no α-hydrogen in BDFP, direct HF elimination is not feasible (vide infra). The experimental activation energy (48 kcal/mol) is much lower than the C–N bond dissociation energy of ~65 kcal/mol observed in some related alkyl mono-difluoroamines [1,4]. These result suggest that the presence of the second NF_2 group in this model compound significantly lowers the dissociation energy of the first C–NF_2 bond.

Summarizing, the experimental kinetic result clearly favors the C–N bond breaking as primary decomposition step although formation of HF and HCN is strongly evident from the FTIR spectra of pyrolyzed BDFP. Their origins will be addressed later.

3.2. Quantum chemical calculations

To elucidate the mechanism for the decomposition of BDFP, we performed ab initio MO and hybrid density-functional calculations. The following three major primary decomposition channels have been identified.

$$\mathrm{BDFP} \rightarrow (\mathrm{CH_3})_2\mathrm{CNF_2} + \mathrm{NF_2} \qquad \text{(I)}$$

$$BDFP \rightarrow CH_3(CH_2)CNF_2 + HNF_2 \quad (II)$$

$$BDFP \rightarrow c{-}CH_3C(CH_2)(NF_2)N(F){-} \quad (III)$$

Reaction channel (I) involves homolytic cleavage of one of the C–NF_2 bonds to form $(CH_3)_2CNF_2$ and NF_2 radicals. The strong electronegative character of F atoms might have a tendency to delocalize the electron from C-center and hence destabilize the radical. In our preliminary study carried out at the B3LYP level with three different basis sets given in Tables 2 and 3, the $(CH_3)_2CNF_2$ radical was found to be unstable. Full optimization of the radical led to an elongation of N–F bond and formation of C–N π bond. This metastable radical, $(CH_3)_2C{=}N(F)$–F, has an elongated N–F bond length of 2.04 Å and is 39.1 kcal/mol higher in energy than BDFP (minus NF_2) at the B3LYP/6-31G(d,p) level of theory. The ''transition state'' TS1 corresponding to the formation of this metastable radical had a barrier of 54.6 kcal/mol with respect to BDFP at the same level of theory. A further single-point energy calculation at B3LYP/6-311+G(3df,2p) lowers the energy to 50.5 kcal/mol. The resultant $(CH_3)_2C{=}NF$ molecule is quite stable and its further decomposition leading to the formation of either $CH_3F + CH_3CN$ or

Table 2
Moments of inertia and vibrational frequencies calculated at the B3LYP/6-31G(d,p) level of theory

Species	I_i (amu)	v_I
BDFP	764, 1455, 1520	76, 109, 184, 198, 206, 289, 292, 326, 336, 370, 447, 506, 518, 556, 679, 774, 823, 907, 925, 965, 985, 1014, 1030, 1046, 1222, 1245, 1273, 1413, 1430, 1496, 1503, 1511, 1524, 3088, 3090, 3172, 3176, 3176, 3176
TS2	805, 1902, 2189	−549, 44, 71, 93, 118, 136, 189, 259, 313, 386, 414, 461, 517, 537, 573, 622, 737, 764, 884, 902, 947, 1009, 1016, 1049, 1058, 1215, 1306, 1401, 1425, 1452, 1480, 1490, 1514, 1720, 3035, 3116, 3119, 3164, 3211
TS3	876, 1510, 1696	−1433, 69, 104, 127, 158, 222, 237, 253, 306, 341, 365, 430, 452, 489, 545, 601, 649, 730, 820, 907, 922, 972, 993, 1003, 1051, 1096, 1202, 1232, 1262, 1391, 1474, 1486, 1498, 1515, 3080, 3145, 3170, 3187, 3236
$(CH_3)_2CNF_2$	401, 531, 886	−34, 85, 89, 235, 287, 367, 418, 462, 502, 758, 853, 872, 964, 986, 996, 1076, 1266, 1299, 1410, 1425, 1479, 1493, 1495, 1508, 2989, 2994, 3099, 3101, 3156, 3158
$CH_3C(CH_2)NF_2$	370, 626, 659	−167, 107, 255, 291, 379, 466, 580, 624, 759, 835, 870, 936, 961, 987, 1038, 1062, 1286, 1418, 1443, 1498, 1503, 1744, 3066, 3127, 3173, 3177, 3271
c–$CH_3C(CH_2)(NF_2)N(F)$–	514, 1125, 1383	76, 148, 184, 251, 290, 328, 354, 472, 478, 522, 615, 717, 829, 862, 907, 932, 949, 1013, 1042, 1098, 1104, 1140, 1266, 1376, 1428, 1477, 1498, 1514, 3077, 3151, 3160, 3185, 3260
$CH_3C(CH_2)NF$	185, 446, 619	96, 243, 328, 384, 481, 536, 574, 795, 882, 970, 993, 1048, 1060, 1329, 1368, 1425, 1498, 1502, 1503, 3058, 3124, 3154, 3191, 3303
$(CH_3)_2CNF$	210, 450, 638	45, 189, 304, 328, 367, 471, 583, 830, 932, 961, 984, 1094, 1115, 1293, 1412, 1422, 1482, 1487, 1488, 1510, 1726, 3045, 3054, 3103, 3107, 3157, 3196
NF_2	26, 154, 180	565, 980, 1119
HNF_2	34, 168, 196	492, 918, 1014, 1322, 1445, 3341
HF	0, 3, 3	4085
$(CH_3)_2C$	43, 195, 217	218, 260, 428, 668, 749, 932, 1016, 1159, 1198, 1342, 1350, 1406, 1412, 1505, 1512, 2928, 2932, 2985, 2986, 3098, 3100
$(CH_3)_2CH(NF_2)$	393, 552, 878	104, 196, 230, 260, 347, 394, 457, 475, 563, 829, 902, 911, 950, 972, 1003, 1154, 1178, 1208, 1357, 1367, 1415, 1433, 1496, 1509, 1509, 1533, 3060, 3060, 3065, 3131, 3137, 3158, 3158
$(CH_3)_2CH$	48, 218, 243	108, 125, 361, 410, 888, 942, 946, 1038, 1154, 1184, 1376, 1423, 1427, 1483, 1493, 1494, 1505, 2952, 2958, 3039, 3041, 3103, 3104, 3179

Table 3
Calculated relative energies with ZPE corrections at different levels of theory based on the optimized geometries with B3LYP/6-31G(d,p) for BDFP decomposition

Species	6-31G(d,p)	6-311G(d,p)	6-311+G(3df,2p)
BDFP	0.00	0.00	0.00
TS2	61.90	59.40	57.13
TS3	78.51	76.84	75.55
$NF_2 + (CH_3)_2CNF_2$	48.58	46.50	43.40
$HNF_2 + CH_3C(CH_2)NF_2$	24.25	18.95	14.23
$HF + CH_3C(CH_2)(NF_2)NF$	−4.40	−11.18	−17.23

cyclic–N=C(CH_3)CH_2– (2-methylazirine) + HF needs to overcome a substantial barrier. The calculated barrier at the B3LYP/6-31G(d,p) level of theory was found to be 81.5 and 69.6 kcal/mol, respectively.

Although the $(CH_3)_2CNF_2$ radical is unstable according to the B3LYP method, it is stable by both Hartree-Fock and MP2 calculations. The calculated C–N bond dissociation energy for the first NF_2 at the B3LYP/6-311+G(3df,2p) level of theory using the geometry optimized at MP2/6-31G(d,p) is 43.4 kcal/mol, which is slightly lower than the values, 48.6 and 46.5 kcal/mol, computed with smaller basis sets 6-31G(d,p) and 6-311G(d,p), respectively. These results are in good agreement with the experimental activation energies, 45–48 kcal/mol mentioned above. A further evaluation of the first C–N bond energy will be made later in conjunction with the rate constant calculation with a variational RRKM theory.

Reaction path (II) involves the elimination of HNF_2 from BDFP through a four-member-ring transition state (TS2). The barrier at TS2 is 57.1 kcal/mol with respect to BDFP at the B3LYP/6-311+G(3df,2p)//B3LYP/6-31G(d,p) level of theory. The substantially higher barrier for this process clearly suggests that it cannot be the primary decomposition pathway for BDFP.

A similarly high-energy barrier is associated with the reaction path (III), the direct HF elimination from a methyl group and the formation of a three-member-ring cyclic intermediate. The calculated barrier at TS3 is 75.6 kcal/mol at the same B3LYP/6-311+G(3df,2p)//B3LYP/6-31G(d,p) level. Thus, reaction path (III) is also unlikely to be an important decomposition pathway for BDFP. The structures of BDFP, all the TSs and other local minima, and the potential energy diagram are shown in Figs. 5 and 6, respectively.

Our theoretical calculation supports the experimental observation of the C–N homolytic bond cleavage as the rate-limiting step for the unimolecular decomposition of BDFP. A variational RRKM calculation of rate constant for this channel (pathway I) must be performed to account for the experimental results as will be discussed below. The formation of HF in the reaction may be attributed to H abstraction by F atoms and/or direct elimination from the $(CH_3)_2CNF_2$ radical as will also be discussed later. HF can further undergo reaction with the quartz wall of the reactor to form SiF_4 as mentioned above. The experimentally observed HCN might result from the secondary decomposition of the $(CH_3)_2CNF_2$ radical, as also concluded by Ross et al [5].

3.3. Varaitional RRKM calculation for k_1

As the unimolecular decomposition of BDFP producing NF_2 and $(CH_3)_2CNF_2$ does not have a well defined transition state, we have calculated its rate constant using the Variflex code of Klippentein and coworkers [15–18]. The potential energy profile required to describe the interaction of the separating fragments was calculated by geometry optimization at different fixed C–N separations in BDFP, covering from 1.6 to 3.4 Å with an interval of 0.1 or 0.2 Å with the smaller interval at the critical separation 2.8–3.4 Å. For each structure, we calculated $3N-7$ vibrational frequencies projected out of the gradient direction. The calculated potential energies at the B3LYP/6-31G(d,p) level of theory were fitted to the Morse potential with $\beta = 2.63$ and $D = 48$ kcal/mol for the E,J-resolved RRKM calculation with the Variflex code [18]. The dissociation energy can be further refined by comparing the predicted rate constant with the experimental result as described below.

The rate constant for the decomposition of BDFP predicted by the variational RRKM calculation is

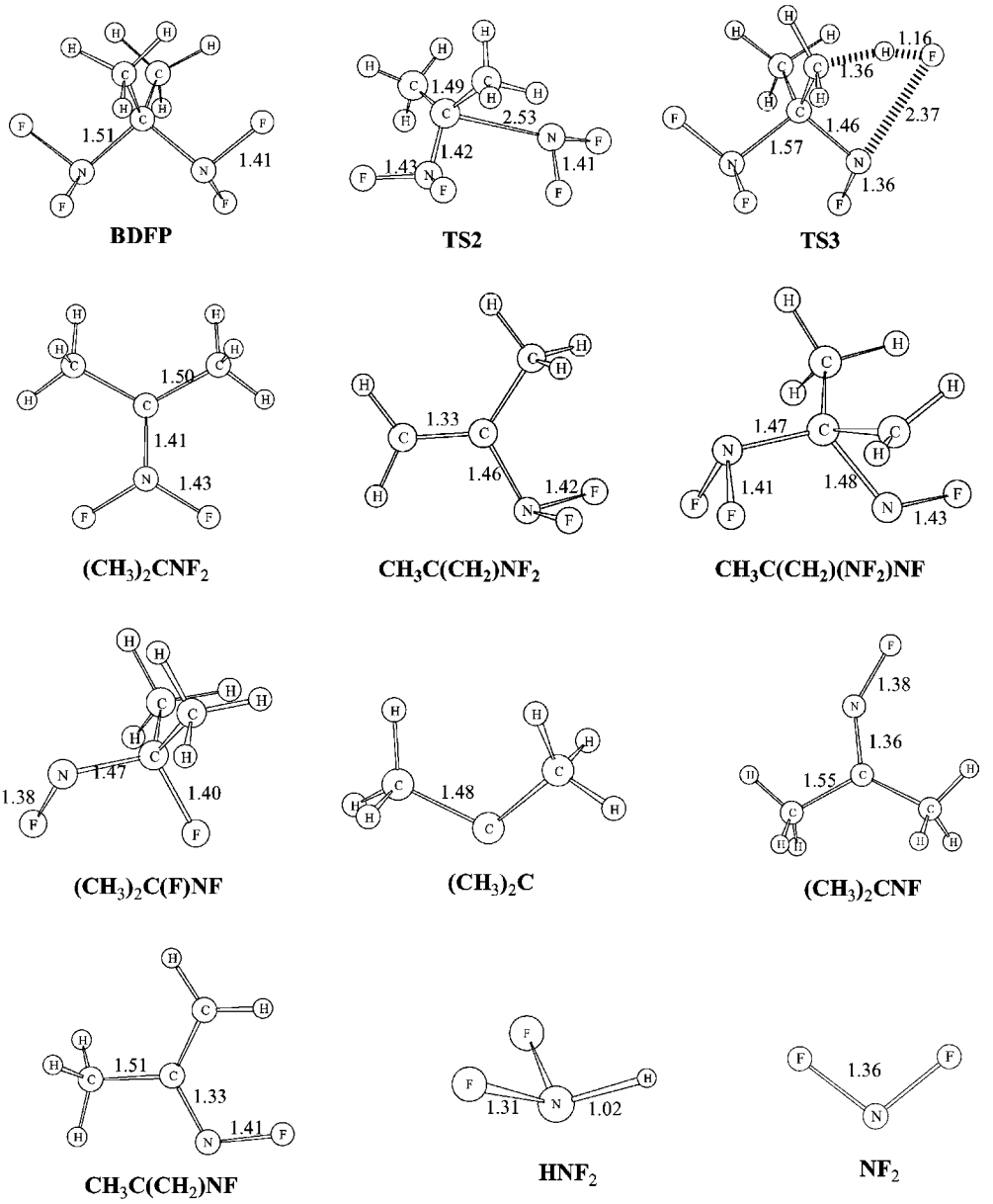

Fig. 5. B3LYP/6-31G(d,p) optimized geometries for the species involved in the decomposition of BDFP and $(CH_3)_2CNF_2$. For simplicity only important parameters are labeled.

shown in Fig. 4 for comparison with the experimentally measured values. As the predicted value depends very strongly on the dissociation energy, which is the least reliable quantity predictable by the B3LYP method (varying from 43.4 to 48.6 kcal/mol), we adjusted the bond dissociation energy initially within the 48 ± 1 kcal/mol range. Final calculations allowed us to bracket the energy within a rather small range of 47.9 ± 0.1 kcal/mol, as illustrated in Fig. 4. The predicted values within the energy range fully encompassed the convoluted experimental errors. The solid line presented in the figure allows us to cover a much

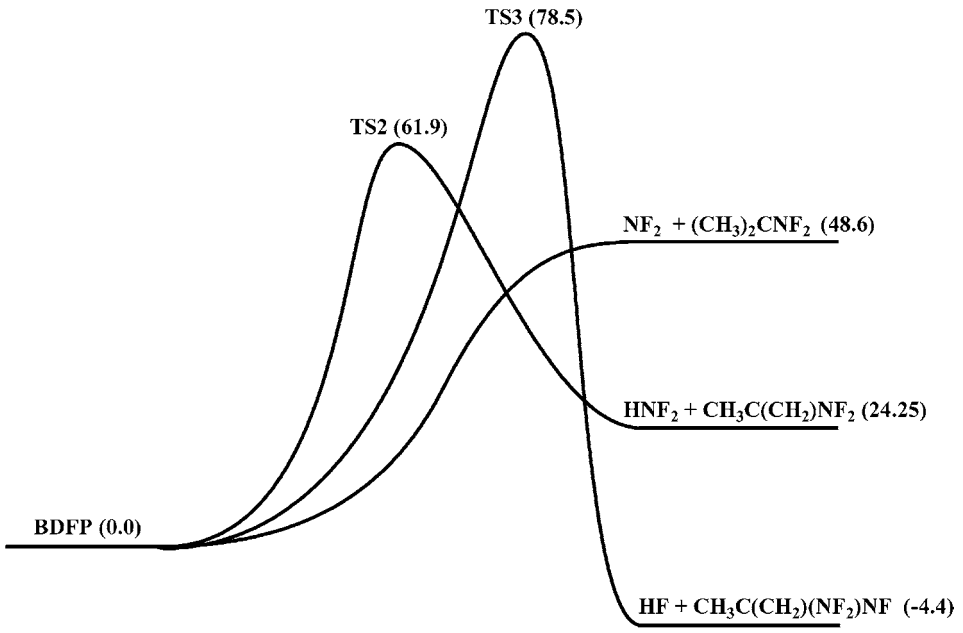

Fig. 6. Calculated potential energy profiles with B3LYP/6-31G(d,p) for the decomposition of BDFP.

wider temperature range (500–2000 K) than can be covered experimentally (493–553 K, including that of Fokin et al. [6]; the theoretical result can be represented by $k_1 = 10^{14.09} \exp(-21860/T)\ s^{-1}$. The significant lowering of the apparent activation energy (from 47.9 to 43.4 kcal/mol) and the associated A-factor results from the effect of angular momentum conservation (i.e. J-dependence) in the dissociation process at higher temperatures.

3.4. Mechanism for $(CH_3)_2CNF_2$ decomposition

The $(CH_3)_2CNF_2$ radical is thermochemically unstable. Since we were unable to find the transition states for the decomposition and isomerization of the $(CH_3)_2CNF_2$ radical by B3LYP or MP2 calculations with basis sets greater than 3-21G(d,p), we studied its reaction mechanism with the geometry optimized at MP2/3-21G(d,p), with additional single-point energy calculations using B3LYP with larger basis sets. The optimized geometry and potential energy profile computed at the MP2/3-21G(d,p) level of theory are shown in Figs. 7 and 8, respectively, and the predicted relative energies are summarized in Table 4.

At the MP2/3-21G(d,p) level, $(CH_3)_2CNF_2$ isomerizes to $(CH_3)_2CFNF$ with a small (7 kcal/mol) barrier at TS1′ ($\nu_i = -825\ cm^{-1}$). The radical can also eliminate to give HF + $CH_3(CH_2)NF$ exothermically ($\Delta H = -29$ kcal/mol) with a small barrier of 16 kcal/mol via a five-centered transition state TS2′ ($\nu_i = -2338\ cm^{-1}$). The small barriers for these unimolecular decomposition reactions are responsible for the thermal instability of the $(CH_3)_2CNF_2$ radical. On the other hand, $(CH_3)_2CNF_2$ decomposes to give F + $(CH_3)_2CNF$ with an unreasonably large 62 kcal/mol barrier (TS3′, $\nu_i = -316\ cm^{-1}$) and 15 kcal/mol exothermicity. It should be noted, however, that the corresponding transition energies calculated by B3LYP//MP2/3-21G(d,p) with larger basis sets are all significantly lower as shown in Table 4.

The decomposition of $(CH_3)_2CFNF$ giving HF + $CH_3(CH_2)CNF$ via a four-centered transition state (TS4′, $\nu_i = -2238\ cm^{-1}$) occurs with a 64 kcal/mol barrier or, equivalently, 15 kcal/mol above $(CH_3)_2CNF_2$, comparable to that of the five-centered TS2′. Since we were unable to find the transition states for the decomposition or isomerization of the $(CH_3)_2CFNF$ giving F + $(CH_3)_2CNF$ at the MP2/3-21G(d,p) level, we obtained its transition state geometry at MP2/3-21G(d) with additional single-point energy calculations using B3LYP with larger basis sets as before. The result shows that $(CH_3)_2CFNF$ decomposes more

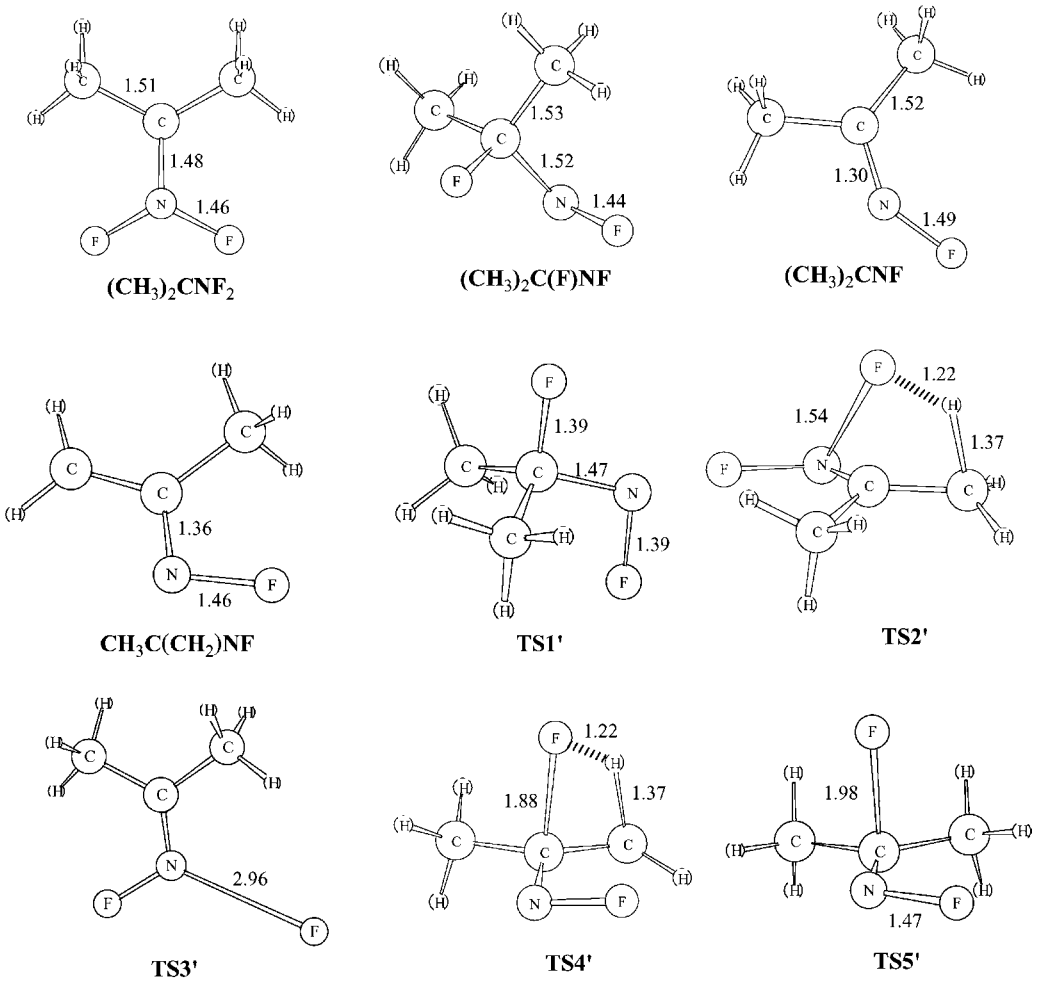

Fig. 7. MP2/3-21G(d,p) optimized geometries for the species involved in the decomposition $(CH_3)_2CNF_2$. For simplicity only important parameters are labeled.

Table 4
Calculated relative energies with ZPE corrections at different levels of theory based on the optimized geometries with MP2/3-21G(d,p) for $(CH_3)_2CNF_2$ radical decomposition

Species	MP2/3-21G(d,p)	B3LYP/6-31G(d,p)	B3LYP/6-311G(d,p)	B3LYP/6-311+G(3df,2p)
$(CH_3)_2CNF_2$	0.00	0.00	0.00	0.00
TS1′	6.99	−6.93	−9.06	−9.78
TS2′	15.99	5.87	3.50	3.51
TS3′	62.08	20.96	17.85	19.64
TS4′	15.48	5.66	3.39	3.14
TS5′[a]	−4.07	−16.33	−20.11	−25.39
$(CH_3)_2CFNF$	−48.66	−47.23	−47.47	−47.43
$NF_2 + (CH_3)_2C$	78.71	69.00	66.83	71.28
$F + (CH_3)_2CNF$	−15.11	0.82	−3.39	−2.84
$HF + CH_3C(CH_2)NF$	−29.37	−38.30	−45.25	−49.90

[a] The relative energies were calculated at different levels of theory based on the optimized geometries with MP2/3-21G(d).

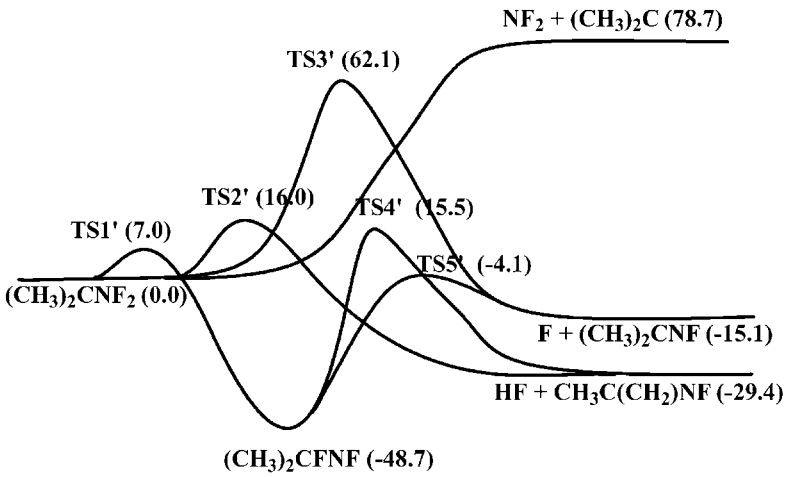

Fig. 8. Calculated potential energy profiles with MP2/3-21G(d,p) for the decomposition of $(CH_3)_2CNF_2$.

readily to give $F + (CH_3)_2CNF$ with a 44 kcal/mol barrier via TS5′ ($v_i = -643\ cm^{-1}$), which lies 4 kcal/mol below $(CH_3)_2CNF_2$ and 66 kcal/mol below TS3′ producing the same products. It is worth noting that a corresponding calculation for TS5′ by B3LYP//MP2/3-21G(d) shows no distinct saddle point with a higher endothermicity of ~45 kcal/mol (above $(CH_3)_2CFNF$). These qualitative results show that $(CH_3)_2CNF_2$ is thermally less stable than its isomer, $(CH_3)_2CFNF$; their decomposition reactions produce F and HF exothermically with respect to the former. The ready formation of F and HF is consistent with the experimental observation of SiF_4 as alluded to before. The HCN absorption peak detected at 713 cm^{-1} in the FTIR spectrum may derive from further decomposition of $CH_3C(CH_2)NF$ producing $CH_2CH + HF +$ HCN, for example. The reaction is estimated to be exothermic by about 3 kcal/mol at the MP2/3-21G(d) level of theory. In addition, HCN could also be formed by the reaction of NF_2 with CH_3, which could be produced by the fragmentation of $(CH_3)_2CFNF$ [5].

The production of NF_2 and $(CH_3)_2C$: diradical from $(CH_3)_2CNF_2$, however, was predicted to be very endothermic (see Table 4), as one would expect. This product channel is not expected to be significant to the overall BDFP pyrolytic chemistry. The results of the quantum chemical calculations as described qualitatively agree with the product distribution reported by Ross et al. [5].

3.5. The C–N bond energy in $(CH_3)_2C(H)NF_2$

The C–N bond energies in several single NF_2-substituted alkanes have been estimated to lie in the range of 62–69 kcal/mol by Sanders and Lin [4] based on the kinetics of NF_2 + olefin reactions. These values are somewhat higher than those predicted by our B3LYP calculations for $(CH_3)_2C(H)NF_2$, 57.1, 55.8 and 54.7 kcal/mol, using 6-31G(d,p), 6-311G(d,p) and 6-311 + G(3df,2p) basis sets, respectively. Comparison of these values with those given in Table 3 for the first C–N bond predicted with the corresponding methods suggests that the presence of the second NF_2 group in the same carbon atom weakens the first C–N bond by about 10 kcal/mol, attributable to the strong electron withdrawing effect of the second group.

4. Conclusion

The results of the thermal decomposition of BDFP using the technique of pyrolysis/FTIR spectrometry indicate for the first time that the breaking of one of the C–NF_2 bonds in this bis-difluoroamino compound is the rate-limiting step. The following first-order rate expression was obtained for the unimolecular decomposition reaction:

$$k_1 = 10^{16.0\pm0.7} \exp\left[-\frac{(24200 \pm 840)}{T}\right] s^{-1}$$

Over the narrow temperature range of 528–553 K. The result agrees excellently with the value reported by Fokin et al. [6], $k_1 = 10^{15.60} \exp(-23600/T)\ s^{-1}$ obtained in the overlapping temperature range, 493–533 K. A variational RRKM (Varilflex) calculation for the rate constant, using the potential energy function computed for the interaction of the NF_2 and $(CH_3)_2CNF_2$ fragments at the B3LYP/6-31G(d,p) level of theory, provides a quantitative agreement with the experimental rate constant as well as the first C–N bond dissociation energy, $D(C–NF_2) = 47.9 \pm 0.1$ kcal/mol.

The $(CH_3)_2CNF_2$ radical has been shown to be unstable; it can decompose readily without significant barriers to give F atoms and HF molecules. The theoretically predicted mechanisms for the decomposition of $(CH_3)_2C(NF_2)_2$ and $(CH_3)_2CNF_2$ agree reasonably with the product distribution reported by Ross et al. [5] based on their low-pressure, high-temperature pyrolysis data.

Acknowledgements

The authors are grateful to the Office of Naval Research for support of this work, under the direction of Dr. J. Goldwasser through ONR grant no. N00014-89-J-1949. We want to take this opportunity to thank Dr. Richard S. Miller for his unwavering support over many years.

References

[1] P. Lane, P. Politzer, Adv. Mol. Struct. Res. 3 (1997) 269.
[2] J.C. Oxley, J.L. Smith, J. Zhang, C. Bedford, J. Phys. Chem. A. 105 (2001) 579.
[3] E.M. Grice, P. Lane, P. Politzer, J. Mol. Struct. 365 (1996) 89.
[4] W.A. Sanders, M.C. Lin, J. Chem. Soc. Faraday Trans. 83 (1987) 905.
[5] D.S. Ross, T. Mill, M.B. Hill, J. Am. Chem. Soc. 94 (1972) 8776.
[6] A.V. Fokin, V.N. Grebennikov, G.B. Manelis, G.M. Nazin, Dokl. Akad. Nauk 332 (1993) 735.
[7] K.J. Baum, Am. Chem. Soc. 90 (1968) 7083.
[8] R.D. Chapman, M.F. Welker, C.B. Kreutzberger, J. Org. Chem. 63 (1998) 1566.
[9] W.H. Graham, J.P. Freeman, J. Org. Chem. 34 (1969) 2589.
[10] A.V. Fokin, Yu.M. Kosyrev, V.A. Makarov, N.P. Novoselov, Doklady Chem. (Eng. Transl.) 186 (1969) 350.
[11] E.A. Lawton, J.Q. Weber, J. Am. Chem. Soc. 85 (1963) 3595.
[12] C.O. Parker, J.P. Freeman, Inorg. Synth. 12 (1970) 307.
[13] K.O. Christe, R.D. Wilson, Inorg. Chem. 26 (1987) 920.
[14] M.T. Bowers, G.I. Kerley, W.H. Flygare, J. Chem. Phys. 45 (1966) 3399.
[15] S.J. Klippenstein, Chem. Phys. Letts. 170 (1990) 71.
[16] S.J. Klippenstein, J. Chem. Phys. 94 (1991) 6469.
[17] S.J. Klippenstein, J. Chem. Phys. 96 (1992) 367.
[18] S.J. Klippenstein, S.H. Robertson, A.F. Wagner, D.M. Wardlaw, Faraday Disc. Chem. Soc. 102 (1995) 65.